I&EC research
Industrial & Engineering Chemistry Research

Article

pubs.acs.org/IECR

Single-Objective and Multiobjective Designs for Hydrogen Networks with Fuel Cells

Yen-Cheng Chiang and Chuei-Tin Chang*

Department of Chemical Engineering, National Cheng Kung University, Tainan 70101, Taiwan

ABSTRACT: Hydrogen network synthesis has always been a popular cost-reduction measure adopted in the petroleum refining industry. Although several mixed-integer nonlinear programming models have already been developed in the past to produce cost-optimal designs, not all relevant units were considered in these studies. In addition, a realistic hydrogen network should clearly be configured on the basis of more than one criterion so as to address both economic and environmental concerns. To circumvent these drawbacks of the available methods, additional unit models for fuel cells and steam reforming plants are incorporated in a comprehensive mathematical program with two objective functions, that is, the total annual cost (TAC) and the global CO_2 emission rate, in the current studies. The trade-off issues between cost reduction and pollution control are addressed by establishing the Pareto front accordingly. Two examples are presented in this paper to demonstrate the feasibility and effectiveness of the proposed approach.

INTRODUCTION

To comply with the increasingly stringent requirements on pollution control, a large amount of hydrogen is consumed in almost every modern petroleum refinery for the purpose of removing sulfur and nitrogen so as to produce on-specification fuels. Although H_2 is the byproduct of catalytic reformer, it is still necessary to operate a supply plant devoted to meet its high demand. On the other hand, in producing and consuming hydrogen, the greenhouse gases (e.g., carbon dioxide) are also generated and emitted in large quantities. Thus, there is an incentive to develop a rigorous and comprehensive mathematical programming model for synthesizing the hydrogen integration scheme that strikes a proper balance between the conflicting design objectives for economic benefit and environmental protection.

In the past, two alternative approaches have been proposed for hydrogen network synthesis, the graphic and model-based methods, and both are aimed toward improving operational efficiency or reducing total annual cost. A brief review of these two typical design strategies is given as follows.

The first systematic approach to integrate hydrogen resources in the refinery was proposed by Towler et al.[1] Later, Alves and Towler[2] applied the so-called "pinch method" to synthesize the H_2 networks. Zhao et al.[3] then extended this design strategy to optimize a multicomponent hydrogen management system, while Ding et al.[4] further introduced pressure considerations so as to ensure feasibility in practice. Finally, Zhang and Feng[5] made use of the graphic method to identify the minimum resource demand in a multicomponent system.

On the other hand, many model-based methods have also been developed in recent years. Hallale and Liu[6] proposed a modeling approach based on a superstructure embedded with pressure constraints. The optimal network design can then be identified by solving this model. Liu and Zhang[7] followed the same approach to optimally place the pressure swing adsorption (PSA) unit(s) for the purpose of improving hydrogen utilization efficiency. Kumar et al.[8] suggested several different models and compared the optimization results. On the basis of the state-space concept, Liao et al.[9] built a mixed integer nonlinear programming (MINLP) model that incorporates component modules for the compressors, PSA units, and hydrogen using units, etc. Ahmad et al.[10] produced flexible H_2 network configurations which are suitable for operation in multiple periods, while Jia and Zhang[11] studied multicomponent hydrogen utilization systems. Jagannath et al.[12] devised an effective algorithm for solving the nonconvex MINLP model used for hydrogen network synthesis. Zhou et al.[13] integrated the H_2 network with a mass exchanger network (MEN) for H_2S removal. To further reduce the overall hydrogen consumption rate, Wu et al.[14] treated the concentrations and flow rates at the sinks as decision variables and also imposed inequality constraints at the inlets of hydrogen users. In a subsequent study, Wu et al.[15] developed two mathematical programming models to determine the minimum energy consumption rate and minimum number of compressors in a hydrogen distribution system, respectively.

The aforementioned studies were basically all concerned with the economic design criteria, while the important issues of carbon emissions were ignored. In a network of hydrogen sources and sinks, the greenhouse gas is emitted mainly from the steam methane reformer (SMR) and the fuel gas system. Additionally, the electricity import required to operate compressors may also be regarded as an indirect emission source. In an attempt to account for both types of emissions with a single performance index, Smith and Delaby[16] proposed to compute a unified "global" emission rate of all possible combinations of utilities and fuels utilized in a process plant. Chang and Hwang[17] later solved a multiobjective optimization problem to identify the most appropriate utility system design

Received: December 2, 2013
Revised: March 13, 2014
Accepted: March 18, 2014
Published: March 18, 2014

dx.doi.org/10.1021/ie404068p | *Ind. Eng. Chem. Res.* 2014, 53, 6006−6020

for any given chemical process. Elkamel et al.[18] considered several different emission reduction measures in their MINLP model to synthesize a refinery production plan that achieves the best compromise between the conflicting objectives for profit taking and pollution control. In a related literature review, Collodi and Wheeler[19] compared various technologies for CO_2 capture in the SMR unit.

From the above review, one can see that a practical hydrogen network may have to be designed with two or more criteria that address both financial and environmental concerns. To this end, a multiobjective version of the available MINLP model and the corresponding solution procedure must be developed to produce a proper network structure. It should also be noted that, although the global carbon emission rate can obviously be reduced by better management of the hydrogen integration system, indirect pollution may be further abated with fuel cells. To be able to consider all design options, it is necessary to build the component models of fuel cell and hydrogen production unit and incorporate them into the conventional formulation.

The remainder of this paper is organized as follows. The mathematical models of all possible units that may be embedded in a hydrogen network are first described in the next section. The third section then delineates the logic constraints for incorporating the options to add new units in a base-case hydrogen network. The objective functions considered in this work, that is, the total annual cost and the global emission rate of carbon dioxide, and their evaluation methods, are presented in the subsequent section. A systematic procedure is then outlined in the fifth section to construct the superstructure for any given hydrogen network synthesis problem. The feasibility and usefulness of the proposed model for generating single- and multiobjective designs are demonstrated with two realistic examples in the next two sections, respectively. Finally, conclusions are drawn and possible future works are discussed at the end of this paper.

UNIT MODELS

To facilitate model formulation, let us first define the following label sets:

$$\mathbf{I} = \{i | i \text{ is the label of a hydrogen source}\}$$

$$\mathbf{J} = \{j | j \text{ is the label of a hydrogen sink}\}$$

The hydrogen plants, hydrocrackers, hydrotreaters, fuel cells, compressors, and pressure swing adsorption unit are regarded as both sources and sinks in this study, while the fuel gas system is obviously only a sink. For the sake of simplicity, let us assume that methane is the only impurity in every hydrogen-containing stream and, also, treat the natural gas supply as a source with 0 vol % hydrogen. The corresponding unit models are briefly listed below:

Hydrogen plant:[20,21]

$$\sum_{i\in\mathbf{I}} F_{i,\mathrm{H2P}} = k \sum_{j\in\mathbf{J}} F_{\mathrm{H2P},j} \tag{1}$$

$$y_{\mathrm{in,H2P}} \sum_{i\in\mathbf{I}} F_{i,\mathrm{H2P}} = \sum_{i\in\mathbf{I}} F_{i,\mathrm{H2P}} y_i \tag{2}$$

$$\sum_{i\in\mathbf{I}} F_{i,\mathrm{H2P}} \le \overline{f}^{\max}_{\mathrm{in,H2P}} \tag{3}$$

$$\sum_{j\in\mathbf{J}} F_{\mathrm{H2P},j} \le \overline{f}^{\max}_{\mathrm{out,H2P}} \tag{4}$$

$$\overline{f}^{\max}_{\mathrm{in,H2P}} = k\overline{f}^{\max}_{\mathrm{out,H2P}} \tag{5}$$

$$y_{\mathrm{in,H2P}} = \overline{y}_{\mathrm{in,H2P}} \tag{6}$$

$$y_{\mathrm{out,H2P}} = \overline{y}_{\mathrm{out,H2P}} \tag{7}$$

$$StMuse = k'' \sum_{j\in\mathbf{J}} F_{\mathrm{H2P},j} \tag{8}$$

$$Q^{\mathrm{H2P}}_{\mathrm{fuel}} = k' \sum_{j\in\mathbf{J}} F_{\mathrm{H2P},j} \tag{9}$$

where $F_{i,\mathrm{H2P}}$ denotes the flow rate of H_2 stream from source i to hydrogen plant H2P (MMscfd); $F_{\mathrm{H2P},j}$ denotes the flow rate of H_2 stream from unit H2P to sink j (MMscfd); $\overline{f}^{\max}_{\mathrm{in,H2P}}$ and $\overline{f}^{\max}_{\mathrm{out,H2P}}$ are model parameters which represent the maximum allowable flow rates of the hydrogen-containing streams (MMscfd) at the inlet and outlet of unit H2P respectively; y_i is the volumetric concentration of hydrogen in source i (vol %); $\overline{y}_{\mathrm{in,H2P}}$ and $\overline{y}_{\mathrm{out,H2P}}$ respectively denote the H_2 concentrations (vol %) at the inlet and outlet of unit H2P and their values are fixed at 30.77 and 99.00 in this study; $StMuse$ (ton/day) and $Q^{\mathrm{H2P}}_{\mathrm{fuel}}$ (MMBTU/day) respectively denote the steam and heat supply rates required in the reforming reaction; k (=0.48), k'(=73.44 BTU/scf), and k'' (=15.48 ton/MMscf) are empirical constants extracted from Rajesh et al.[20] and Posada and Manousiouthakis.[21]

Hydrogen user:[6]

$$\sum_{i\in\mathbf{I}} F_{i,\mathrm{cs}} = \overline{f}_{\mathrm{in,cs}} \tag{10}$$

$$\sum_{i\in\mathbf{I}} F_{i,\mathrm{cs}} y_i = \overline{f}_{\mathrm{in,cs}}\, y_{\mathrm{in,cs}} \tag{11}$$

$$\sum_{j\in\mathbf{J}} F_{\mathrm{cs},j} = \overline{f}_{\mathrm{out,cs}} \tag{12}$$

$$y_{\mathrm{in,cs}} = \overline{y}_{\mathrm{in,cs}} \tag{13}$$

$$y_{\mathrm{out,cs}} = \overline{y}_{\mathrm{out,cs}} \tag{14}$$

where cs $\in$ **CS**, and **CS** respectively represent the set of hydrogen users (e.g., hydrocrackers and hydrotreaters); $F_{i,}$ denotes the flow rate of H_2 stream from source i to unit (MMscfd); F_j denotes flow rate of H_2 stream from unit to sink j (MMscfd); $\overline{f}_{\mathrm{in,cs}}$ and $\overline{f}_{\mathrm{out,cs}}$ are model parameters which represent the flow rates of H_2 streams (MMscfd) at the inlet and outlet of unit respectively; $\overline{y}_{\mathrm{in,cs}}$ and $\overline{y}_{\mathrm{out,cs}}$ are model parameters which respectively denote the H_2 concentrations (vol %) at the inlet and outlet of unit .

Fuel cell:[22,23]

$$y_{\mathrm{in,fc}} \sum_{i\in\mathbf{I}} F_{i,\mathrm{fc}} = \sum_{i\in\mathbf{I}} F_{i,\mathrm{fc}} y_i \tag{15}$$

$$\mathrm{power}_{\mathrm{fc}} = \eta_{\mathrm{fc}} \mathrm{LHV}_{\mathrm{H_2}} \frac{\overline{\rho}^{\circ}_{\mathrm{H_2}}}{\mathrm{M}_{\mathrm{H_2}}} \sum_{i\in\mathbf{I}} F_{i,\mathrm{fc}} y_i \tag{16}$$

$$(1-\mu_{\mathrm{fc}}) \sum_{i\in\mathbf{I}} F_{i,\mathrm{fc}} y_i = y_{\mathrm{out,fc}} \sum_{j\in\mathbf{J}} F_{\mathrm{fc},j} \tag{17}$$

dx.doi.org/10.1021/ie404068p | Ind. Eng. Chem. Res. 2014, 53, 6006−6020

$$\eta_{fc} = \frac{\mu_{fc} v_c}{1.25} \tag{18}$$

$$\sum_{i \in \mathbf{I}} F_{i,fc} y_i \le \overline{fy}^{max}_{in,fc} \tag{19}$$

$$y_{in,fc} \ge \overline{y}^{min}_{in,fc} \tag{20}$$

$$y_{out,fc} = \overline{y}_{out,fc} \tag{21}$$

where fc ∈ **FC** and **FC** represents the set of fuel cells; $F_{i,fc}$ denotes the flow rate of H_2 stream from source i to unit fc (MMscfd); $F_{fc,j}$ denotes the flow rate of H_2 stream from unit fc to sink j (MMscfd); $\overline{fy}^{max}_{in,fc}$ is the maximum allowable hydrogen feed rate of fuel cell fc, whose value is set to be 180 MMscfd in this study; $y_{in,fc}$ denotes the H_2 concentration (vol %) at the inlet of fuel cell fc; the $\overline{y}^{min}_{in,fc}$ (= 99.95 vol %) and $\overline{y}_{out,fc}$ (= 99.95 vol %) are both model parameters which respectively denote the lower bound of H_2 concentrations at the inlet and the fixed H_2 concentration at the outlet of fuel cell fc; $power_{fc}$ is the power generated by fuel cell fc (MW); η_{fc} is the electrical conversion efficiency of fuel cell fc, and its value should be between 0.55 and 0.60; μ_{fc} denotes the fuel utilization rate of fuel cell fc and its value should be between 0.86 and 0.94; v_c is the operating voltage of fuel cell and a value of 0.8 (volt) has been chosen in the present study; $\overline{\rho}^{o}_{H_2}$ is the density of hydrogen under standard conditions, that is, 0.003 lb/scf; M_{H_2} denotes the molecular weight of hydrogen, that is, 2.02 g/mol; LHV_{H_2} is the lower heating value of hydrogen, and its value 229.25 BTU/mol.

Note that the solid oxide fuel cell (SOFC), which utilizes high-purity hydrogen as the raw material, is incorporated in the proposed superstructure to analyze the merits of converting chemical energy to electricity. Equations 15 and 20 are adopted mainly to impose a lower bound on the hydrogen concentration at the inlet of the fuel cell. Equations 16 and 18 are used for estimating the SOFC-generated power. Equations 17 and 18 also define the fuel utilization rate and the electrical conversion efficiency, respectively, and the latter is set at 0.6 in this study. Equation 19 gives the upper limit of hydrogen throughput, while eq 21 fixes the outlet concentration of hydrogen.

Fuel gas system:[6]

$$Q_{fuel} = \Delta H^{o}_{c,H_2} \frac{\overline{\rho}^{o}_{H_2}}{M_{H_2}} \sum_{i \in \mathbf{I}} F_{i,fuel} y_i + \Delta H^{o}_{c,CH_4} \frac{\overline{\rho}^{o}_{CH_4}}{M_{CH_4}} \sum_{i \in \mathbf{I}} F_{i,fuel}(1 - y_i) \tag{22}$$

where Q_{fuel} denotes the total heat generation rate of the fuel gas system (MMBTU/day); $F_{i,fuel}$ denotes the flow rate of H_2 stream from source i to the fuel gas system (MMscfd); $\overline{\rho}^{o}_{CH_4}$ is the density of methane under standard conditions, that is, 0.024 lbm/scf; M_{CH_4} denotes the molecular weight of methane, that is, 16.04 g/mol; $\Delta H^{o}_{c,H_2}$ (= 229.25 BTU/mol) and $\Delta H^{o}_{c,CH_4}$ (= 760.88 BTU/mol) denote the heats of combustion of hydrogen and methane, respectively.

Compressor:[6]

$$\sum_{j \in \mathbf{J}} F_{com,j} = \sum_{i \in \mathbf{I}} F_{i,com} \tag{23}$$

$$y_{com} \sum_{j \in \mathbf{J}} F_{com,j} = \sum_{i \in \mathbf{I}} F_{i,com} y_i \tag{24}$$

$$\sum_{i \in \mathbf{I}} F_{i,com} \le \overline{f}^{max}_{in,com} \tag{25}$$

$$\eta_{com} power_{com} = \left(\left(\frac{P^{out}_{com}}{P^{in}_{com}} \right)^{\gamma_{com} - 1/\gamma_{com}} - 1 \right) \times TC_{p,com} \rho^{o}_{com} \sum_{i \in \mathbf{I}} F_{i,com} \tag{26}$$

$$\rho^{o}_{com} = \frac{\overline{\rho}^{o}_{H_2}}{M_{H_2}} y_{com} + \frac{\overline{\rho}^{o}_{CH_4}}{M_{CH_4}} (1 - y_{com}) \tag{27}$$

$$C_{p,com} \rho^{o}_{com} = C_{p,H_2} \frac{\overline{\rho}^{o}_{H_2}}{M_{H_2}} y_{com} + C_{p,CH_4} \frac{\overline{\rho}^{o}_{CH_4}}{M_{CH_4}} (1 - y_{com}) \tag{28}$$

$$\gamma_{com} = 1 + \left(\frac{y_{com}}{\gamma_{H_2} - 1} + \frac{1 - y_{com}}{\gamma_{CH_4} - 1} \right)^{-1} \tag{29}$$

where com ∈ **COM** and **COM** represents the set of compressors; $F_{i,com}$ denotes the flow rate of H_2 stream from source i to compressor com (MMscfd); $\overline{f}^{max}_{in,com}$ is a model parameter that represents the maximum allowable throughput (MMscfd) of compressor com; y_{com} denotes the H_2 concentration (vol %) at the exit of compressor com; $power_{com}$ is the power (MW) required in operating compressor com; $C_{p,com}$ is the heat capacity (kJ/(mol-K)) of the stream entering compressor com; γ_{com} is the heat capacity ratio (-) of the stream entering compressor com; ρ^{o}_{com} is the molar density (mol/scf) of the stream entering compressor com under standard conditions; P^{in}_{com} and P^{out}_{com} denote the suction and discharge pressures (psi) of compressor com, respectively; T is the compressor inlet temperature (which is set to be constant at 298.15 K); η_{com} is compressor efficiency (which is fixed at 0.8 in this study). In this compressor model, the thermodynamic properties of hydrogen and methane are assumed to be constants and their values are listed below:

- C_{p,H_2} = 0.0288 (kJ/(mol-K)); γ_{H_2} = 1.42 (-)
- C_{p,CH_4} = 0.0357 (kJ/(mol-K)); γ_{CH_4} = 1.30 (-)

Pressure swing adsorption column:[6]

$$y_{in,pur} \sum_{i \in \mathbf{I}} F_{i,pur} = \sum_{i \in \mathbf{I}} F_{i,pur} y_i \tag{30}$$

$$y^{prod}_{pur} \sum_{j \in \mathbf{J}} F^{prod}_{pur,j} = R \sum_{i \in \mathbf{I}} F_{i,pur} y_i \tag{31}$$

$$\sum_{i \in \mathbf{I}} F_{i,pur} = \sum_{j \in \mathbf{J}} F^{prod}_{pur,j} + \sum_{j \in \mathbf{J}} F^{resid}_{pur,j} \tag{32}$$

$$\sum_{i \in \mathbf{I}} F_{i,pur} y_i = y^{prod}_{pur} \sum_{j \in \mathbf{J}} F^{prod}_{pur,j} + y^{resid}_{pur} \sum_{j \in \mathbf{J}} F^{resid}_{pur,j} \tag{33}$$

dx.doi.org/10.1021/ie404068p | Ind. Eng. Chem. Res. 2014, 53, 6006−6020

$$\sum_{i\in\mathbf{I}} F_{i,\mathrm{pur}} y_i \le \overline{fy}^{\max}_{\mathrm{in,pur}} \tag{34}$$

$$y_{\mathrm{in,pur}} \ge \overline{y}^{\min}_{\mathrm{in,pur}} \tag{35}$$

$$y^{\mathrm{prod}}_{\mathrm{pur}} \ge \overline{y}^{\min}_{\mathrm{out,pur}} \tag{36}$$

where pur ∈ **PUR** and **PUR** denotes the set of all available PSAs; $F_{i,\mathrm{pur}}$ denotes the flow rate of H_2 stream from source i to PSA unit pur (MMscfd); $F^{\mathrm{prod}}_{\mathrm{pur},j}$ denotes the flow rate of product stream from PSA unit pur to sink j (MMscfd); $F^{\mathrm{resid}}_{\mathrm{pur},j}$ denotes the flow rate of residue stream from PSA unit pur to sink j (MMscfd); $\overline{fy}^{\max}_{\mathrm{in,pur}}$ is the maximum allowable processing rate of hydrogen in PSA unit pur, whose value is set to be 200 MMscfd in this study; $y_{\mathrm{in,pur}}$ denotes the H_2 concentration (vol %) at the inlet of PSA unit pur; the $\overline{y}^{\min}_{\mathrm{in,pur}}$ (= 80.0 vol %) is a model parameter which represents the lower bound of H_2 concentrations at the inlet of PSA unit pur; $y^{\mathrm{resid}}_{\mathrm{pur}}$ and $y^{\mathrm{prod}}_{\mathrm{pur}}$, respectively, denote the volumetric concentrations (vol %) of hydrogen in the product and residue streams of PSA unit pur; $\overline{y}^{\min}_{\mathrm{out,pur}}$ (=99.95 vol %) is the lower bound of $y^{\mathrm{prod}}_{\mathrm{pur}}$; R (=0.9) is a dimensionless constant representing the hydrogen recovery ratio.

Options for Extra Units. It is assumed in this study that a conventional structure (in which the raw-material supplies, the hydrogen plant, the hydrogen users, and the fuel gas system are connected sequentially with compressors) can always be made available by using an ad hoc synthesis approach either for a revamp application or for a new design. To facilitate construction of an optimal hydrogen network, one or more extra units, for example, compressors, PSAs, and fuel cells, may have to be incorporated. For the purpose of providing such options in optimization studies, it is necessary to impose the following inequality constraints in the proposed model:

$$e_{\mathrm{neq}} B^{F_{\mathrm{neq}}}_{\mathrm{lo}} \le \sum_{i\in\mathbf{I}} F_{i,\mathrm{neq}} \le e_{\mathrm{neq}} B^{F_{\mathrm{neq}}}_{\mathrm{up}} \quad \forall\ \mathrm{neq} \in \mathbf{NEQ} \tag{37}$$

where **NEQ** denotes the set of all extra units; $e_{\mathrm{neq}} \in \{0,1\}$ is a binary variable reflecting if unit neq is present in the optimal structure; $B^{F_{\mathrm{neq}}}_{\mathrm{up}}$ and $B^{F_{\mathrm{neq}}}_{\mathrm{low}}$ denote the upper and lower bound of inlet flow rate of unit neq, respectively. In this study, only extra compressors, PSAs, and fuel cells can be selected to augment the existing units in the conventional structure. Specifically, let us use the symbols **COM**′ ⊂ **COM**, **PUR**′ ⊂ **PUR** and **FC**′ ⊂ **FC** to denote the sets of extra compressors, PSAs, and fuel cells, respectively, and therefore, **NEQ** = **COM**′ ∪ **PUR**′ ∪ **FC**′. Furthermore, if there is a need to limit the numbers of additional compressors, PSAs, and fuel cells that must be purchased, the following inequalities should also be included in the model

$$\sum_{\mathrm{com}\in\mathbf{COM}'} e_{\mathrm{com}} \le N_{\mathrm{comp}} \tag{38}$$

$$\sum_{\mathrm{pur}\in\mathbf{PUR}'} e_{\mathrm{pur}} \le N_{\mathrm{pur}} \tag{39}$$

$$\sum_{\mathrm{fc}\in\mathbf{FC}'} e_{\mathrm{fc}} \le N_{\mathrm{fc}} \tag{40}$$

where N_{comp}, N_{pur}, and N_{fc} are designer-specified parameters for setting the maximum numbers of extra compressors, PSAs, and fuel cells, respectively.

DESIGN OBJECTIVES

Two design objectives can be adopted in the proposed mathematical programming model, that is, the total annual cost (TAC) and the global emission rate of carbon dioxide. The corresponding objective functions are illustrated as follows:

Total annual cost:[6,22−25] The total annual cost (TAC) is the sum of annual operating cost and the annualized capital cost, i.e.

$$\mathrm{TAC} = \text{annual operating cost} + \mathrm{Af} \times \text{capital cost} \tag{41}$$

In this equation, Af is the annualization factor computed according to the following formula:

$$\mathrm{Af} = \frac{\mathrm{fi}(1+\mathrm{fi})^{\mathrm{ny}}}{(1+\mathrm{fi})^{\mathrm{ny}} - 1} \tag{42}$$

where fi is the interest rate and ny is the service life of the hydrogen network (years).

The annual operating cost is determined in this study by considering the costs incurred due to the needs to consume natural gas, steam and power (for operating the compressors), the revenues generated from thermal energy produced by burning the tail gases, and from electricity produced by the fuel cells, and the cost required to operate and maintain the fuel cells:

$$\text{annual operating cost} = \mathrm{cost}_{\mathrm{NG}} + \mathrm{cost}_{\mathrm{StM}} + \mathrm{cost}_{\mathrm{comp}} - \mathrm{Rvn}_{\mathrm{exFuel}} - \mathrm{Rvn}_{\mathrm{fc}} + \mathrm{cost}_{\mathrm{OM\text{-}fc}} \tag{43}$$

The terms on the right side of this equation (million $/year) can be expressed as

$$\mathrm{cost}_{\mathrm{NG}} = \mathrm{oyU}_{\mathrm{NG}} \sum_{j\in\mathbf{J}} F_{\mathrm{NG},j} \tag{44}$$

$$\mathrm{cost}_{\mathrm{StM}} = \mathrm{oyU}_{\mathrm{StM}} StMuse \tag{45}$$

$$\mathrm{cost}_{\mathrm{comp}} = \mathrm{oyU}_{\mathrm{power}} \sum_{\mathrm{com}\in\mathbf{COM}} \mathrm{power}_{\mathrm{com}} \tag{46}$$

$$\mathrm{Rvn}_{\mathrm{exFuel}} = \mathrm{oyU}_{\mathrm{exFuel}} (Q_{\mathrm{fuel}} - Q^{\mathrm{H2P}}_{\mathrm{fuel}}) \tag{47}$$

$$\mathrm{Rvn}_{\mathrm{fc}} = \mathrm{oyU}_{\mathrm{Power}} \sum_{\mathrm{fc}\in\mathbf{FC}} \mathrm{power}_{\mathrm{fc}} \tag{48}$$

$$\mathrm{cost}_{\mathrm{OM\text{-}fc}} = \mathrm{oyOM}_{\mathrm{fc}} \sum_{\mathrm{fc}\in\mathbf{FC}} \mathrm{power}_{\mathrm{fc}} \tag{49}$$

where oy denotes the total operating time per year and its value is 8000 h/year; U_{NG} denotes the unit cost of natural gas and its value is 5000 $/MMscf; U_{StM} denotes the unit cost of steam and its value is 10 $/ton; U_{exFuel} denotes the unit price of thermal energy and its value is 5 $/MMBtu; $\mathrm{OM}_{\mathrm{fc}}$ denotes the unit cost for operating and maintaining the fuel cell and its value is 0.016 $/kW-h. Note that all other variables in the above equations can be determined on the basis of the unit models described previously.

On the other hand, the capital investments needed for building an optimal hydrogen network are associated with the additional compressors, PSAs, and fuel cells that must be purchased to complement the existing units, that is, the total capital cost can be expressed as

$$\text{capital cost} = C_{\mathrm{comp}} + C_{\mathrm{pur}} + C_{\mathrm{fc}} \tag{50}$$

dx.doi.org/10.1021/ie404068p | Ind. Eng. Chem. Res. 2014, 53, 6006−6020

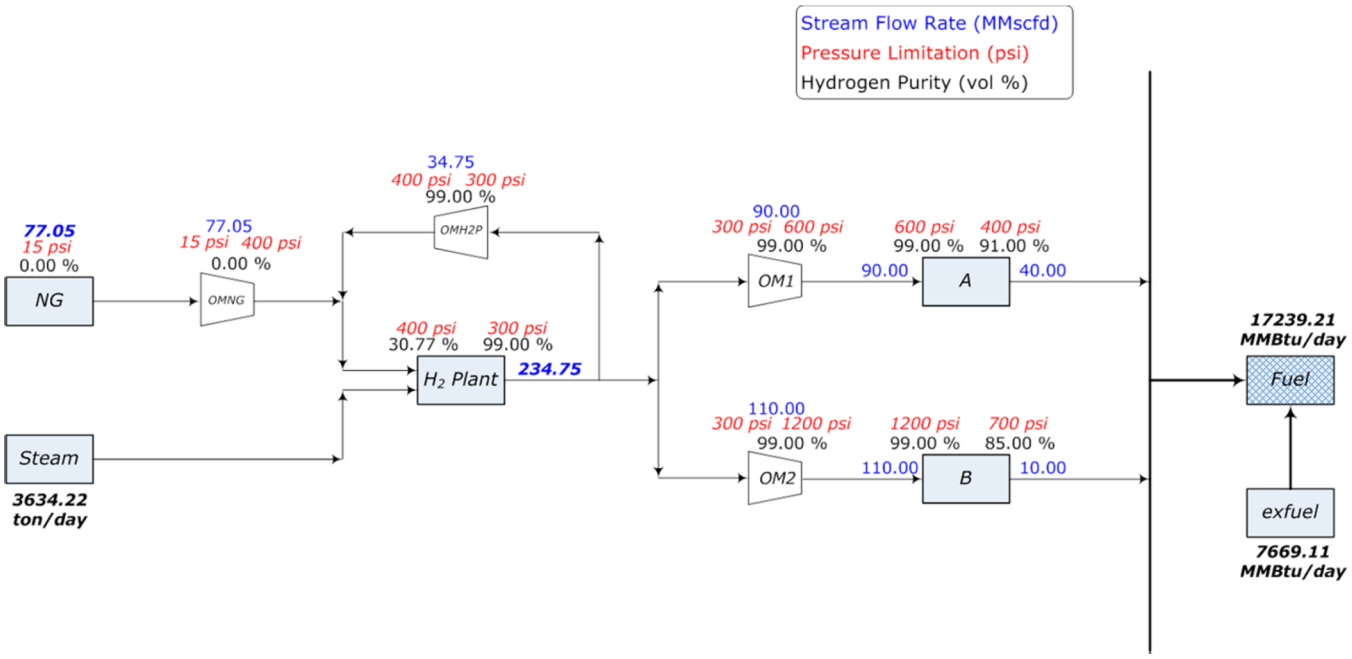

Figure 1. The base-case design in Example 1.

The individual capital costs in this equation can be computed with the following cost models:

$$C_{\text{comp}} = \sum_{\text{com}\in\mathbf{COM}'} e_{\text{com}}(a_{\text{com}} + b_{\text{com}}\text{power}_{\text{com}}) \tag{51}$$

$$C_{\text{pur}} = \sum_{\text{pur}\in\mathbf{PUR}'} e_{\text{pur}}(a_{\text{pur}} + b_{\text{pur}} \sum_{i\in\mathbf{I}} F_{i,\text{pur}}) \tag{52}$$

$$C_{\text{fc}} = \sum_{\text{fc}\in\mathbf{FC}'} e_{\text{fc}} a_{\text{fc}} \text{power}_{\text{fc}} \tag{53}$$

where $\mathbf{COM}' \subset \mathbf{COM}$, $\mathbf{PUR}' \subset \mathbf{PUR}$, and $\mathbf{FC}' \subset \mathbf{FC}$ denote the sets of extra compressors, PSAs, and fuel cells, respectively, and the corresponding cost coefficients are listed below:

1. $a_{\text{com}} = 178.83$ (k$), $b_{\text{com}} = 2.97$ (k$/kW)
2. $a_{\text{pur}} = 666.34$ (k$), $b_{\text{pur}} = 459.48$ (k$/kW)
3. $a_{\text{fc}} = 2242.99$ (k$)

Global CO_2 emission rate:[16,22,23,26] In this study, the *global emission rate* of CO_2 caused by operating the hydrogen network is adopted as another objective function. Specifically, this rate (denoted as *GCems*) is calculated on the basis of the following formula:

$$\begin{aligned} GCems = {} & \text{Local emission rate} \\ & + \left\{\begin{array}{l}\text{Emission rate from the remote}\\ \text{central power station corresponding}\\ \text{to the amount of electricity}\\ \text{imported}\end{array}\right\} \\ & - \left\{\begin{array}{l}\text{Emission rate saved at the remote}\\ \text{central power station corresponding}\\ \text{to the amount of electricity}\\ \text{exported from the site}\end{array}\right\} \end{aligned} \tag{54}$$

The local emissions can be primarily attributed to those generated in the hydrogen production unit and also the fuel gas system:

$$\text{local emission rate} = Ems_{\text{H2P}} + Ems_{\text{Tfuel}} \tag{55}$$

In the former case, the emission rate is

$$Ems_{\text{H2P}} = \text{oyS}_{\text{H2P}} \bar{\rho}^{\circ}_{\text{H}_2} y_{\text{out,H2P}} \sum_{j\in\mathbf{J}} F_{\text{H2P},j} \tag{56}$$

where S_{H2P} is the emission coefficient of the hydrogen production plant and its value is 7.33 (kg CO_2/kg H_2). The emission rate of the fuel gas system is computed on the basis of the assumptions that the tail gases in the fuel gas system are oxidized completely and the only other component in fuel gas is methane, that is,

$$Ems_{\text{Tfuel}} = \text{oyM}_{\text{CO}_2}\left[\frac{\bar{\rho}^{\circ}_{\text{CH}_4}}{\text{M}_{\text{CH}_4}} \sum_{i\in\mathbf{I}} F_{i,\text{fuel}}(1 - y_i) + e_{\text{f}} \frac{(Q^{\text{H2P}}_{\text{fuel}} - Q_{\text{fuel}})}{\Delta H^{\circ}_{c,\text{CH}_4}}\right] \tag{57}$$

It should be noted that, if the heating energy required in the hydrogen plant exceeds that generated by burning tail gases in the fuel gas system, an extra amount of fuel must be consumed to make up for the difference. To account for this additional emission, a binary variable e_{f} is introduced in the second term on the right side of eq 57 and the following two logic constraints are also imposed accordingly:

$$Q^{\text{H2P}}_{\text{fuel}} - Q_{\text{fuel}} - e_{\text{f}} B^{\text{Q}}_{\text{up}} \le 0 \tag{58}$$

$$Q^{\text{H2P}}_{\text{fuel}} - Q_{\text{fuel}} + (1 - e_{\text{f}}) B^{\text{Q}}_{\text{up}} \ge B^{\text{Q}}_{\text{lo}} \tag{59}$$

where B^{Q}_{up} and B^{Q}_{lo}, respectively, denote the upper and lower bounds of the aforementioned energy difference. An estimate of the largest $Q^{\text{H2P}}_{\text{fuel}}$ has been used in the former case, while a very small positive value (say 0.01) has been used for the latter.

dx.doi.org/10.1021/ie404068p | Ind. Eng. Chem. Res. 2014, 53, 6006−6020

Finally, the indirect emissions outside the hydrogen system can be accounted for by computing Ems_{power} with the formula given below:

$$Ems_{power} = oyS_{pc}\left(\sum_{com\in \mathbf{COM}} power_{com} - \sum_{fc\in \mathbf{FC}} power_{fc}\right) \quad (60)$$

where S_{pc} is the emission coefficient of the remote power plant and a value of 0.56 (kg CO_2/(kW-h)) is adopted in this work.

SUPERSTRUCTURES

Similar to any other optimization study in process synthesis, it is necessary to first build a superstructure to facilitate model formulation. The collection of all feasible links between hydrogen sources (i.e., the unit outlets) and sinks (i.e., the unit inlets) is considered as a superstructure in this work. Three connection rules should be followed to build this structure: (1) A source-sink link can be established if the corresponding pressure drop is non-negative. (2) If the sink of a connection is associated with the suction side of a compressor, then its discharge pressure should not be lower than that of the source. (3) Any self-recycle stream around a compressor is not allowed.

For the sake of illustration clarity, let us use the hydrogen network in Figure 1 as an example (which is referred to as Example 1 in this paper) and assume that its structure was configured with an ad hoc approach to connect the existing units in a refinery, that is, a steam supply, a natural gas (NG) supply, a H_2 production plant (H2P), two hydrogen users (A and B), a fuel gas system, and four compressors (OM1, OM2, OMNG, and OMH2P). Note that these units are organized sequentially in a logical order and, also, that the tail gases of units A and B in this base-case design are not recycled and reused. The compressor capacities and their suction and discharge pressures can be found in in Tables 1 and 2,

Table 1. Capacities of the Existing Compressors in Example 1

	OM1	OM2	OMNG	OMH2P
$\overline{f}^{max}_{in,com}$ (MMscfd)	99.00	121.00	84.76	38.33

Table 2. Suction and Discharge Pressures of the Existing Compressors in Example 1

compressor	P^{in}_{com} (psi)	P^{out}_{com} (psi)
OM1	300	600
OM2	300	1200
OMNG	15	400
OMH2P	300	400

respectively. The temperature, pressure, and maximum flow rate of steam supply are respectively set to be 893.5 K, 400 psi, and 4644.3 ton/day, while the pressure, hydrogen concentration, and maximum NG supply rate are assumed to be 15 psi, 0 vol % and 120 MMscfd, respectively. The operating conditions of the other hydrogen sources and sinks in this process are listed in Tables 3 and 4, respectively. By fixing the network structure, the operating conditions in Figure 1 and Table 5 can be obtained by solving the optimization problem corresponding to the objective function of total annual cost (TAC).

On the basis of the above process data, the feasible links among existing units in the superstructure can be established by

Table 3. Operating Conditions of Hydrogen Sources in Example 1

unit	flow rate (MMscfd)	purity (vol %)	pressure (psi)
A	40.00[a]	91.00[d]	400
B	10.00[b]	85.00[e]	700
H2P	300.00[c]	99.00[f]	300

[a] $\overline{f}_{out,A}$. [b] $\overline{f}_{out,B}$. [c] $\overline{f}^{max}_{out,H2P}$. [d] $\overline{y}_{out,A}$. [e] $\overline{y}_{out,B}$. [f] $\overline{y}_{out,H2P}$.

Table 4. Operating Conditions of Hydrogen Sinks in Example 1

process	flow rate (MMscfd)	purity (vol %)	pressure (psi)
A	90.00[a]	99.00[d]	600
B	110.00[b]	99.00[e]	1200
H2P	142.89[c]	30.77[f]	400

[a] $\overline{f}_{in,A}$. [b] $\overline{f}_{in,B}$. [c] $\overline{f}^{max}_{in,H2P}$. [d] $\overline{y}_{in,A}$. [e] $\overline{y}_{in,B}$. [f] $\overline{y}_{in,H2P}$.

Table 5. Power Requirements of Compressors in the Conventional Design of Example 1

	OM1	OM2	OMNG	OMH2P
power (MW)	1.71	4.67	9.08	0.26

applying the connection rules (see the solid lines in Figure 2). Note that not all source-sink pairs are selected. For example, although the link between unit B (source) and OMH2P (sink) satisfies the first connection rule, it is nonetheless excluded due to rule 2. On the other hand, it should be noted that the operating pressures of the extra units should be properly specified so as to optimize the chosen performance indices of a hydrogen network. Let us try to produce an exhaustive list of alternatives for every such unit in the above example:

Fuel cells: For simplicity, let us assume that only the solid oxide fuel cells (SOFC) are available and the inlet and outlet pressures are all roughly around 100 psi.

PSAs: Literature survey suggests that the feed and product pressures of a PSA do not differ significantly and both should be controlled between 150 and 1000 psig. On the other hand, the residue pressure is quite low and, for simplicity, it has been set arbitrarily to one tenth of the feed pressure in this study. On the basis of these principles, all candidates for a new PSA can be identified from the operating pressures of existing sources in the above example (see Table 6). Thus, for every extra PSA under consideration, the following constraint should be imposed:

$$\sum_{pp\in \mathbf{PP}_{pur}} e_{pur,pp} \le e_{pur} \quad \forall\ pur \in \mathbf{PUR}' \quad (61)$$

where $\mathbf{PP}_{pur}$ is the set of all alternative operating pressures for the PSA unit pur (e.g., see the four options in Table 6); $e_{pur,pp} \in \{0,1\}$ is a binary variable used to reflect if the ppth pressure combination is chosen to operate unit pur.

Compressors: Basically, an extra compressor can always be installed between a low-pressure source and a high-pressure sink. Thus, from the aforementioned source and sink pressures associated with the existing units and the extra fuel cells and PSAs, one can identify all possible combinations of suction and discharge pressures of a new compressor. Table 7 shows the list of all such candidate pressures adopted in Example 1. For each extra compressor to be added in optimal design, the following constraint should be included in the mathematical programming model:

dx.doi.org/10.1021/ie404068p | Ind. Eng. Chem. Res. 2014, 53, 6006−6020

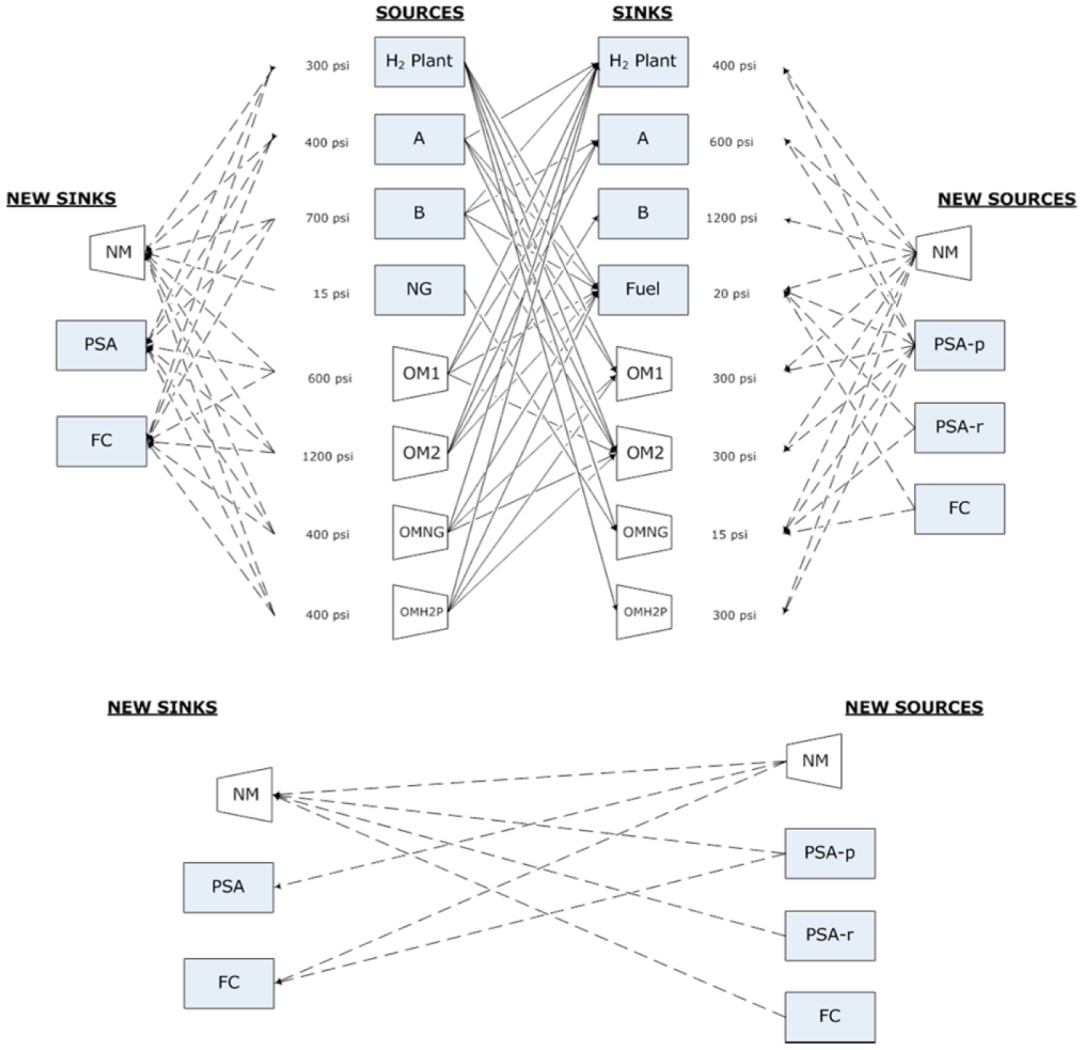

Figure 2. The superstructure in Example 1.

Table 6. Alternative Operating Pressures of a New PSA in Example 1

no.	P^{in}_{pur} (psi)	$P^{out,proud}_{pur}$ (psi)	$P^{out,resid}_{pur}$ (psi)
1	400	400	40
2	700	700	70
3	300	300	30
4	600	600	60

Table 7. Alternative Operating Pressures of a New Compressor in Example 1

no.	P^{in}_{com} (psi)	P^{out}_{com} (psi)	No.	P^{in}_{com} (psi)	P^{out}_{com} (psi)
1	400	600	12	15	1200
2	400	1200	13	15	400
3	400	700	14	15	300
4	700	1200	15	15	100
5	300	600	16	15	700
6	300	1200	17	100	600
7	300	400	18	100	1200
8	300	700	19	100	400
9	600	1200	20	100	300
10	600	700	21	100	700
11	15	600			

$$\sum_{pp \in \mathbf{PP}_{com}} e_{com,pp} \le e_{com} com \in \mathbf{COM}' \quad (62)$$

where $\mathbf{PP}_{com}$ is the set of all pressure alternatives for compressor com (e.g., see the 21 candidates in Table 7); $e_{com,pp} \in \{0,1\}$ is a binary variable used to reflect if the ppth suction-discharge pressure pair is chosen to operate compressor com.

If a source−sink link in the superstructure involves one or two extra units, it is qualitatively represented by a dotted line in Figure 2. This link still must satisfy the connection rules and thus may or may not be present for a specific selection of pressure combinations.

■ SINGLE-OBJECTIVE DESIGNS

The advantages of adopting a superstructure-based synthesis strategy can be clearly demonstrated by comparing the resulting single-objective designs with those generated by the conventional ad hoc approach. On the basis of the aforementioned model formulation, a total of 276 specific constraints were constructed with 697 variables for the hydrogen network in Example 1. The two objective functions mentioned previously, that is, the total annual cost (TAC) and the global CO_2 emission rate, were considered in two separate case studies. The corresponding MINLP models were solved on an Intel

dx.doi.org/10.1021/ie404068p | Ind. Eng. Chem. Res. 2014, 53, 6006−6020

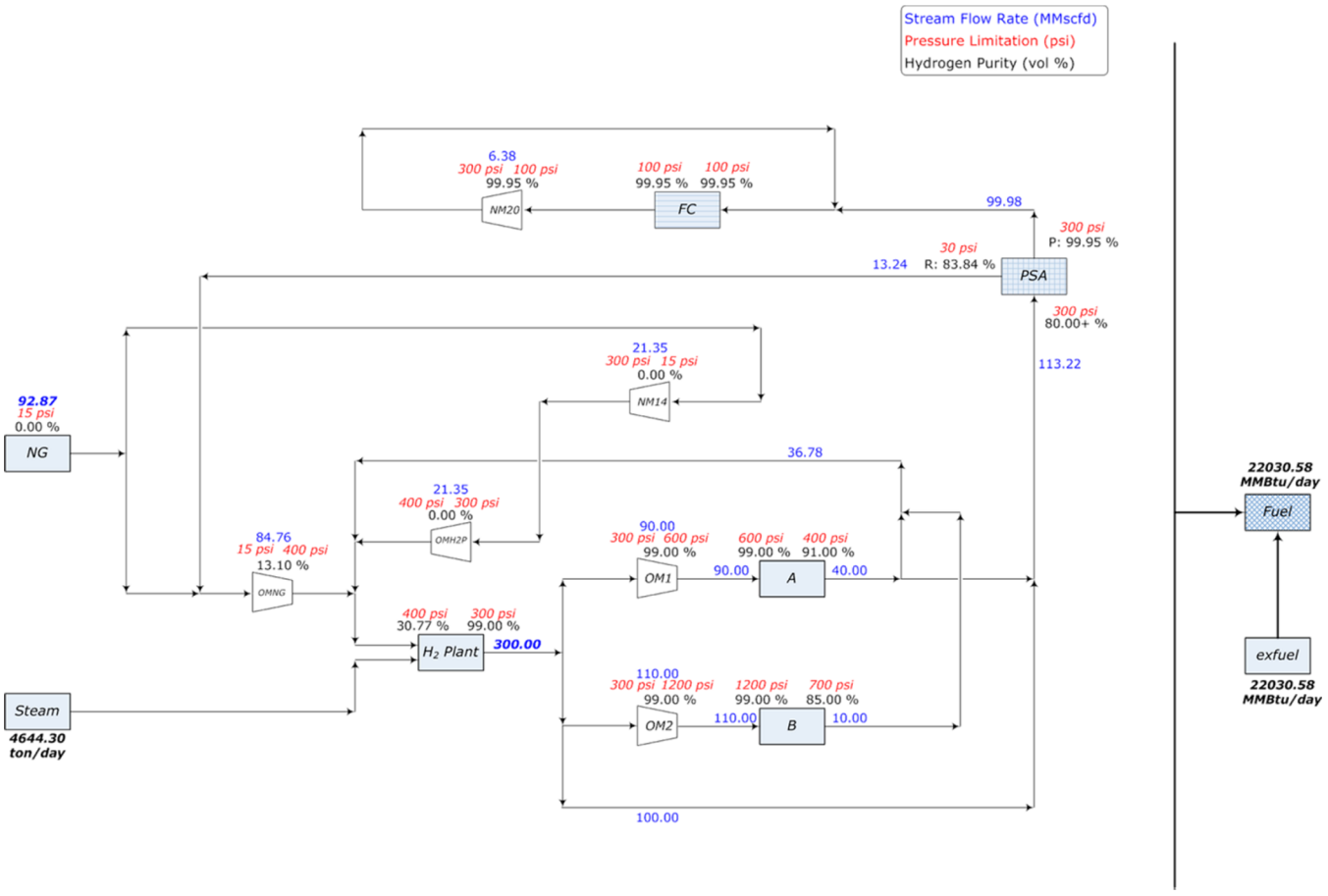

Figure 3. The cost-optimal design in Example 1.

Core i7-2600 3.40 GHz PC with the DICOPT module, together with the MIP solver CPLEX and the NLP solver CONOPT, in the GAMS environment (version 23.7.3). To ensure solution quality, the optimization problem in each case has been solved repeatedly in 3000 independent runs with randomly generated initial guesses. Notice that this approach is adopted mainly on the grounds that BARON was found to be computationally inefficient for the present applications.

By allowing one extra PSA, one extra fuel cell (η_{fc} = 0.60), and two extra compressors, and also assuming that the annual interest rate is 5% and the operation life of every extra unit is 7 years, the best results obtained in two case studies are presented below, respectively:

1. Minimum Total Annual Cost. Each run in this case took about 2.4 s to converge, and the resulting cost-optimal network is given in Figure 3. Note that, in this structure, the tail gases of the hydrogen users, the exhaust stream of the fuel cell and the residue stream of PSA are all recycled. As a result, an additional amount of external fuel is needed in the fuel gas system to provide the heat required for running the hydrogen plant. The tail gas of unit A is delivered to the PSA and also to the hydrogen plant, while that of unit B is reused only for H_2 production. Other than the recycled stream from unit A, the product of the hydrogen plant is also partly utilized as the raw material of PSA so as to produce enough on-spec feed for the fuel cell (FC). The electricity generated by the fuel cell (120.52 MW) is consumed by the compressors for driving the H_2 network and, also, exported for a profit. Since the hydrogen content in the residue flow of PSA is still quite significant, it is recycled to the H_2 plant to avoid depreciating its value in the fuel gas system. Note also that there are two new compressors, NM20 and NM14. The former is used to recycle and reuse the exhaust stream of fuel cell, while the latter is used to raise the supply capacity of natural gas. Finally, the power requirement of every compressor in this hydrogen network can be found in Table 8.

Table 8. Powers Requirements of Compressors in the Cost-Optimal Design in Example 1

	OM1	OM2	OMNG	OMH2P	NM14	NM20
power (MW)	1.71	4.67	10.15	0.15	2.21	0.21

Cost breakdowns for the cost-optimal design in this case are given in Table 9, while the contributions to the global CO_2 emission rate can be found in Table 10. For comparison purposes, the corresponding optimization results obtained on the basis of the conventional structure in Figure 1 are also listed in these two tables. Notice that the total cost and emission levels of the cost-optimal design can both be improved, respectively, to about 24.1% and 8.0% lower than those achieved in the conventional design. Note also from the third row in Table 9 that the negative electricity expenditure of the proposed design, that is $cost_{comp} - Rvn_{fc} < 0$ in eq 43, indicates that the extra fuel cell is capable of not only satisfying the internal power consumptions but also gaining profit via electricity sales. As a result, it is possible to save 56.5% of the total operating cost needed for running the conventional

dx.doi.org/10.1021/ie404068p | Ind. Eng. Chem. Res. 2014, 53, 6006−6020

Table 9. Cost Breakdowns of the Conventional, Cost-Optimal and Emission-Optimal Designs in Example 1 (million $/year)

	conventional network	cost-optimal network	emission-optimal network
natural gas	128.43	154.77	91.55
steam	12.11	15.48	9.37
electricity	22.64	−146.04	18.44
fuel	−12.78	−36.72	−22.22
O&M of fuel cell	0.00	15.55	0.00
operating cost	175.96	76.48	141.58
compressor	0.00	1.30	2.93
PSA	0.00	9.11	1.77
fuel cell	0.00	46.72	0.00
annual capital cost	0.00	57.13	4.70
TAC	175.96	133.61	146.28

Table 10. Contributions to CO_2 Emissions Associated with the Conventional, Cost-Optimal and Emission-Optimal Designs in Example 1 (ton/day)

	conventional network	cost-optimal network	emission-optimal network
H_2 plant	2117.02	2705.41	1636.95
fuel	543.62	1163.71	704.12
electric power	192.97	−1244.79	157.15
global CO_2 emissions rate	2853.61	2624.33	2498.22

network. On the other hand, since an additional amount of external fuel is needed in the cost-optimal design, the corresponding revenue listed in the fourth row in Table 9 should be negative, that is, $Rvn_{exFuel} < 0$ in eq 43. Finally, the negative emission rate caused by power generation (see the third row in Table 10) is obviously due to the excess electricity generated by fuel cell and consumed by external users, that is, $Ems_{power} < 0$ in eq 60.

2. Minimum Global CO_2 Emission Rate. Each run in this case took about 2.7 s to converge, and the resulting emission-optimal network is sketched in Figure 4. It should be noted first that *not* all available units are needed in the proposed design. Specifically, two existing compressors, OMH2P and OM2, and the new fuel cell are excluded. The optimal network is assembled only with the other existing units, two extra compressors (NM5 and NM9) and one extra PSA. Note that, in this structure, since the tail gases of the hydrogen users and the residue stream of PSA are recycled, an additional amount of external fuel must be consumed in the fuel gas system to provide the heat required for running the hydrogen plant. The tail gas of unit A is directed to the PSA and also to the hydrogen plant, while that of unit B is entirely sent to PSA. The high-purity product of PSA is split into two and then recycled back to unit A and unit B, respectively. Since the hydrogen content in the residue flow of PSA is still quite high, it is recycled to the H_2 plant to avoid depreciating its value in the fuel gas system. The new compressor NM5 is adopted mainly to facilitate flows from the hydrogen plant to both unit A and unit B, while NM9 further raises the pressure of feed stream to the latter. The existing compressor OM1 is used to direct the tail gas of unit A to PSA, while OMNG feeds the H_2 plant with natural gas. Finally, the power requirement of every compressor in this hydrogen network can be found in Table 11.

Table 11. Powers Requirements of Compressors in the Emission-Optimal Design in Example 1

	OM1	OM2	OMNG	OMH2P	NM5	NM9
power (MW)	0.20	0.00	7.01	0.00	3.50	2.10

The cost breakdowns and emission contributions obtained in the present case are also listed in Table 9 and Table 10, respectively. Since an additional amount of external fuel is needed in the emission-optimal design, the corresponding revenue in Table 9 should also be negative. Consequently, the CO_2 emission rate from the fuel gas system in the emission-

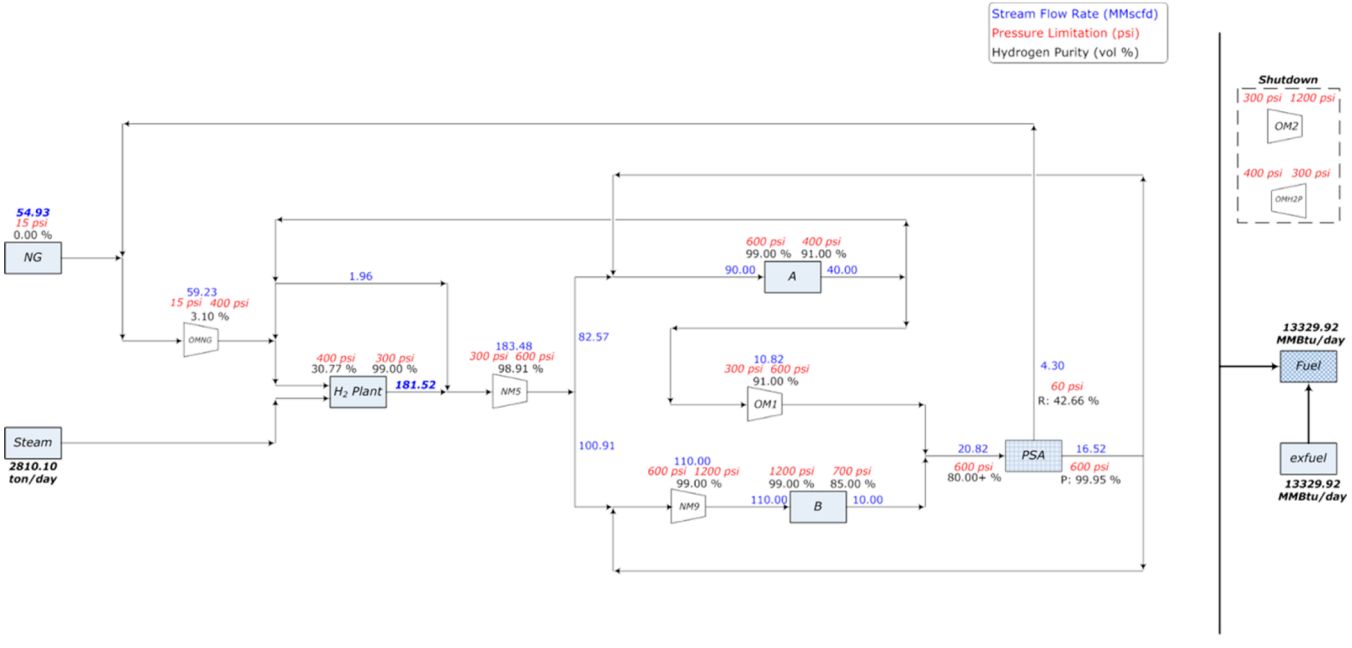

Figure 4. The emission-optimal design in Example 1.

dx.doi.org/10.1021/ie404068p | Ind. Eng. Chem. Res. 2014, 53, 6006−6020

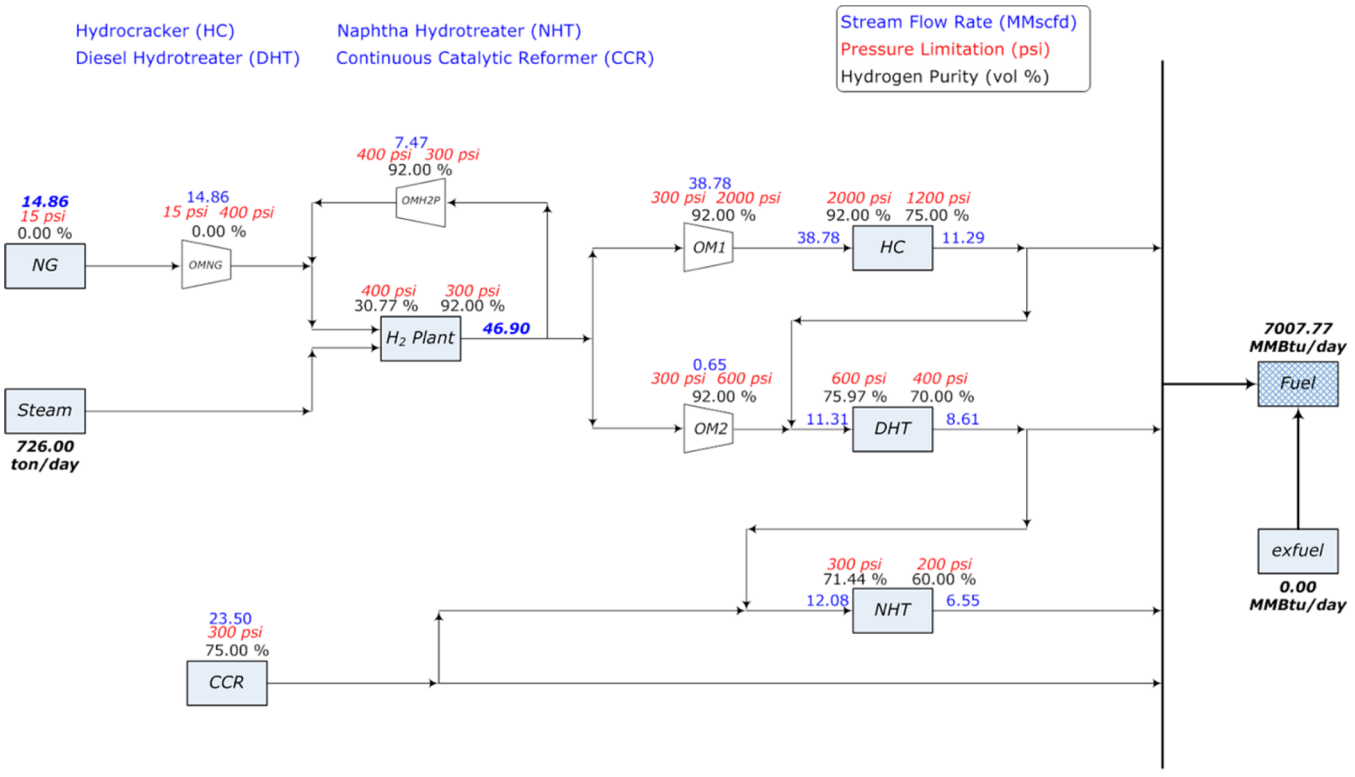

Figure 5. The base-case design in Example 2.

optimal design is higher than that of the conventional design (see Table 10). However, it should also be noted that the throughput of hydrogen plant can now be reduced to 77.3% of the conventional level, which results in considerable decreases in the consumption rates of natural gas, steam, and electricity. As a result, the total emission rate of carbon dioxide can be cut down significantly. When compared with the conventional design, the TAC and global emission rate of the emission-optimal structure can be improved to 83.1% and 87.5% of the base-case values, respectively.

MULTIOBJECTIVE DESIGNS

From the aforementioned optimum solutions of the single-objective models, one can see that it may not always be possible to optimize two (or more) performance measures simultaneously. Specifically, when one target is reached, the other aspects of design may be far from satisfactory. The proper trade-off among competing objectives is really dependent upon

Table 12. Capacities of the Existing Compressors in Example 2

	OM1	OM2	OMNG	OMH2P
$\bar{f}^{max}_{in,com}$ (MMscfd)	40.72	0.68	16.35	8.22

Table 13. Suction and Discharge Pressures of the Existing Compressors in Example 2

compressor	P^{in}_{com} (psi)	P^{out}_{com} (psi)
OM1	300	2000
OM2	300	600
OMNG	15	400
OMH2P	300	400

Table 14. Operating Conditions of Hydrogen Sources in Example 2

process	flow rate (MMscfd)	purity (vol %)	pressure (psi)
HC	11.29[a]	75.00[e]	1200
DHT	8.61[b]	70.00[f]	400
NHT	6.55[c]	60.00[g]	200
H2P	65.00[d]	92.00[h]	300

[a] $\bar{f}_{out,HC}$. [b] $\bar{f}_{out,DHT}$. [c] $\bar{f}_{out,NHT}$. [d] $\bar{f}^{max}_{out,H2P}$. [e] $\bar{y}_{out,HC}$. [f] $\bar{y}_{out,DHT}$. [g] $\bar{y}_{out,NHT}$. [h] $\bar{y}_{out,H2P}$.

Table 15. Operating Conditions of Hydrogen Sinks in Example 2

process	flow rate (MMscfd)	purity (vol %)	pressure (psi)
HC	38.78[a]	92.00[e]	2000
DHT	11.31[b]	75.97[f]	600
NHT	12.08[c]	71.44[g]	300
H2P	30.96[d]	30.77[h]	400

[a] $\bar{f}_{in,HC}$. [b] $\bar{f}_{in,DHT}$. [c] $\bar{f}_{in,NHT}$. [d] $\bar{f}^{max}_{in,H2P}$. [e] $\bar{y}_{in,HC}$. [f] $\bar{y}_{in,DHT}$. [g] $\bar{y}_{in,NHT}$. [h] $\bar{y}_{in,H2P}$.

Table 16. Power Requirements of Compressors in the Conventional Design of Example 2

	OM1	OM2	OMNG	OMH2P
power (MW)	2.42	0.01	1.75	0.06

Table 17. Alternative Operating Pressures of a New PSA in Example 2

no.	P^{in}_{pur} (psi)	$P^{out,prod}_{pur}$ (psi)	$P^{out,resid}_{pur}$ (psi)
1	400	400	40
2	200	200	20
3	300	300	30
4	600	600	60

dx.doi.org/10.1021/ie404068p | Ind. Eng. Chem. Res. 2014, 53, 6006−6020

Table 18. Alternative Operating Pressures of a New Compressor in Example 2

no.	P^{in}_{com} (psi)	P^{out}_{com} (psi)	no.	P^{in}_{com} (psi)	P^{out}_{com} (psi)
1	1200	2000	12	100	200
2	400	2000	13	300	2000
3	400	600	14	300	600
4	200	2000	15	300	400
5	200	600	16	600	2000
6	200	300	17	15	2000
7	200	400	18	15	600
8	100	2000	19	15	300
9	100	600	20	15	100
10	100	300	21	15	400
11	100	400	22	15	200

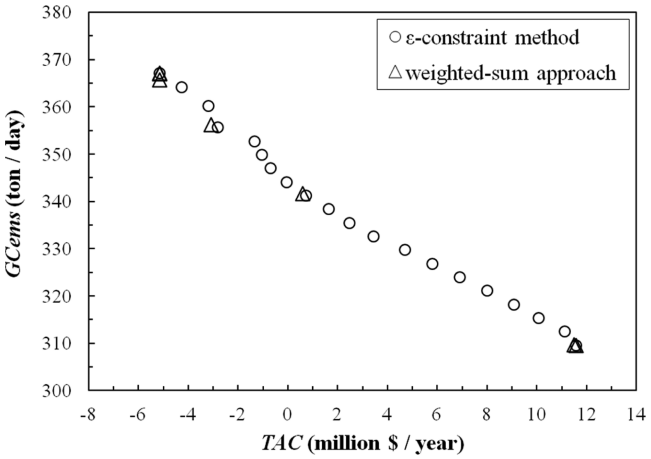

Figure 6. The Pareto front in Example 2.

Table 19. Pareto Front Generated with the ε-Constrained Method in Example 2

no.	TAC ($/year)	*GCems* (ton/year)	no.	TAC ($/year)	*GCems* (ton/year)
1	−5158440.00	367.12	12	2471770.00	335.51
2	−4286660.00	364.25	13	3429100.00	332.63
3	−3199530.00	360.22	14	4699276.00	329.76
4	−2617600.00	358.50	15	5793775.00	326.88
5	−2830000.00	355.63	16	6888356.00	324.01
6	−1356120.00	352.75	17	7983022.00	321.13
7	−1064710.00	349.88	18	9077797.00	318.26
8	−697067.00	347.00	19	10067770.00	315.39
9	−46856.30	344.13	20	11099360.00	312.51
10	706508.20	341.25	21	11560850.00	309.64
11	1627455.00	338.38			

the *preference* of the decision maker(s). If one can identify a common measure of effectiveness by means of which each of the objectives can be expressed, it should be possible to aggregate all of them into an equivalent function and solve the resulting problem with a traditional optimization approach. However, in the present application, it is difficult to justify the implied assumption that the two objectives are commensurable. First of all, to convert the environmental impacts into equivalent financial implications is not a trivial task. Further, this approach itself, that is, to express pollution problems solely in terms of monetary losses, is still highly controversial. Therefore, from the standpoint of a design engineer, it seems reasonable to generate a collection of solutions along the Pareto front before making the final decision. Two available algorithms have been adopted for this purpose, the weighted-sum method[27] and the ε-constrained method.[28,29] In the former case, the objective functions are first normalized and then aggregated into one by assigning various combinations of weights to account for their contributions. The aggregated objective functions can be optimized with any traditional algorithm. On the other hand, the latter method requires repeated optimization of only one of the given objectives while imposing different upper limits on the other. For the sake of brevity, the detailed descriptions of these methods are omitted in this paper. Let us instead use a second example to demonstrate the benefits of multiobjective designs in the sequel.

Figure 5 shows the base-case design adopted in this example, which is essentially the modified version of a structure taken from Hallale and Liu.[6] The existing units in this network include: a steam supply, a natural gas supply (NG), a H_2 plant, a continuous catalytic reformer (CCR), a hydrocracker (HC), a diesel hydrotreater (DHT), a naphtha hydrotreater (NHT), a fuel gas system, and four compressors (OM1, OM2, OMNG, OMH2P). Note that these units are also organized sequentially in the base-case structure and the tail gases of the hydrogen users (HC, DHT and NHT) and the CCR unit are used (at least partially) as fuels for generating heating energy. The compressor capacities and their suction and discharge pressures can be found in Table 12 and 13, respectively. The temperature, pressure, and maximum supply rate of steam are set to be 893.5 K, 400 psi, and 1006.3 ton/day, respectively. The pressure, hydrogen concentration, and maximum flow rate of natural gas supply are assumed to be 15 psi, 0 vol % and 30 MMscfd, respectively, while those of the CCR product are kept at 300 psi, 75 vol % and 23.5 MMscfd, respectively. The operating conditions of the other sources and sinks in this process are listed in Tables 14 and 15. With a fixed base-case configuration, the operating conditions in Figure 5 and Table 16 can be obtained by minimizing the total annual cost (TAC). Note that in this case the heating energy generated in the fuel gas system is more than enough for running the hydrogen plant (which requires only 3443.84 MMBTU/day) and, also, the consumption rates of steam and natural gas are lower than the upper limits of their supply rates.

Let us assume that, because of space limitation in the plant, it is only possible to install at most one extra PSA, two extra compressors, and two extra fuel cells. The efficiency (η_{fc}) and maximum power output ($\overline{power}_{fc}$) of one new fuel cell are assumed to be 0.6 and 15 MW, respectively, while those of another are set at 0.55 and 20 MW, respectively. Note also that the maximum power output can be computed according to eqs 16 and 19:

$$\overline{power}_{fc} = \eta_{fc} LHV_{H_2} \frac{\bar{\rho}^{o}_{H_2}}{M_{H_2}} \overline{fy}^{max}_{in,fc} \tag{63}$$

A 20-year operation life and 5% interest rate of these units have been chosen in this example to compute the annualized capital costs of these units. Finally, in order to build the superstructure, the pressure combinations of the extra PSA and compressors have been identified and listed in Tables 17 and 18, respectively.

As mentioned before, both the weighted-sum method and the ε-constrained method have been used to generate the multiobjective designs. From the resulting Pareto front plotted

dx.doi.org/10.1021/ie404068p | Ind. Eng. Chem. Res. 2014, 53, 6006−6020

Table 20. Cost Breakdowns of the Conventional and Five Multiobjective Designs in Example 2 (million $/year)

	Pareto-optimal solutions					
conventional network		no. 2	no. 6	no. 11	no. 15	no. 19
natural gas	24.77	18.83	15.04	11.03	6.93	2.78
steam	2.42	3.29	2.82	2.32	1.81	1.30
electricity	6.11	−48.92	−37.18	−25.03	−12.23	0.72
fuel	5.94	−7.80	−6.69	−5.51	−4.30	−3.09
O&M of fuel cell	0.00	5.05	3.95	2.79	1.61	0.41
operating cost	27.36	−13.95	−8.68	−3.38	2.42	8.30
compressor	0.00	0.67	0.50	0.05	0.06	0.05
PSA	0.00	1.96	1.31	1.06	1.06	1.13
fuel cell	0.00	7.04	5.51	3.90	2.25	0.58
annual capital cost	0.00	9.67	7.32	5.01	3.37	1.76
TAC	27.36	−4.28	−1.36	1.63	5.79	10.06

Table 21. Contributions to CO_2 Emissions Associated with the Conventional and Five Multiobjective Designs Example 2 (ton/day)

	new network (Pareto-optimal solution)					
original network		no. 2	no. 6	no. 11	no. 15	no. 19
H_2 plant	393.01	534.06	457.75	377.18	294.75	211.39
fuel	211.43	247.20	211.88	174.59	136.43	97.84
electric power	52.05	−417.01	−316.88	−213.39	−104.30	6.15
global CO_2 Emissions Rate	656.49	364.25	352.75	338.38	326.88	315.38

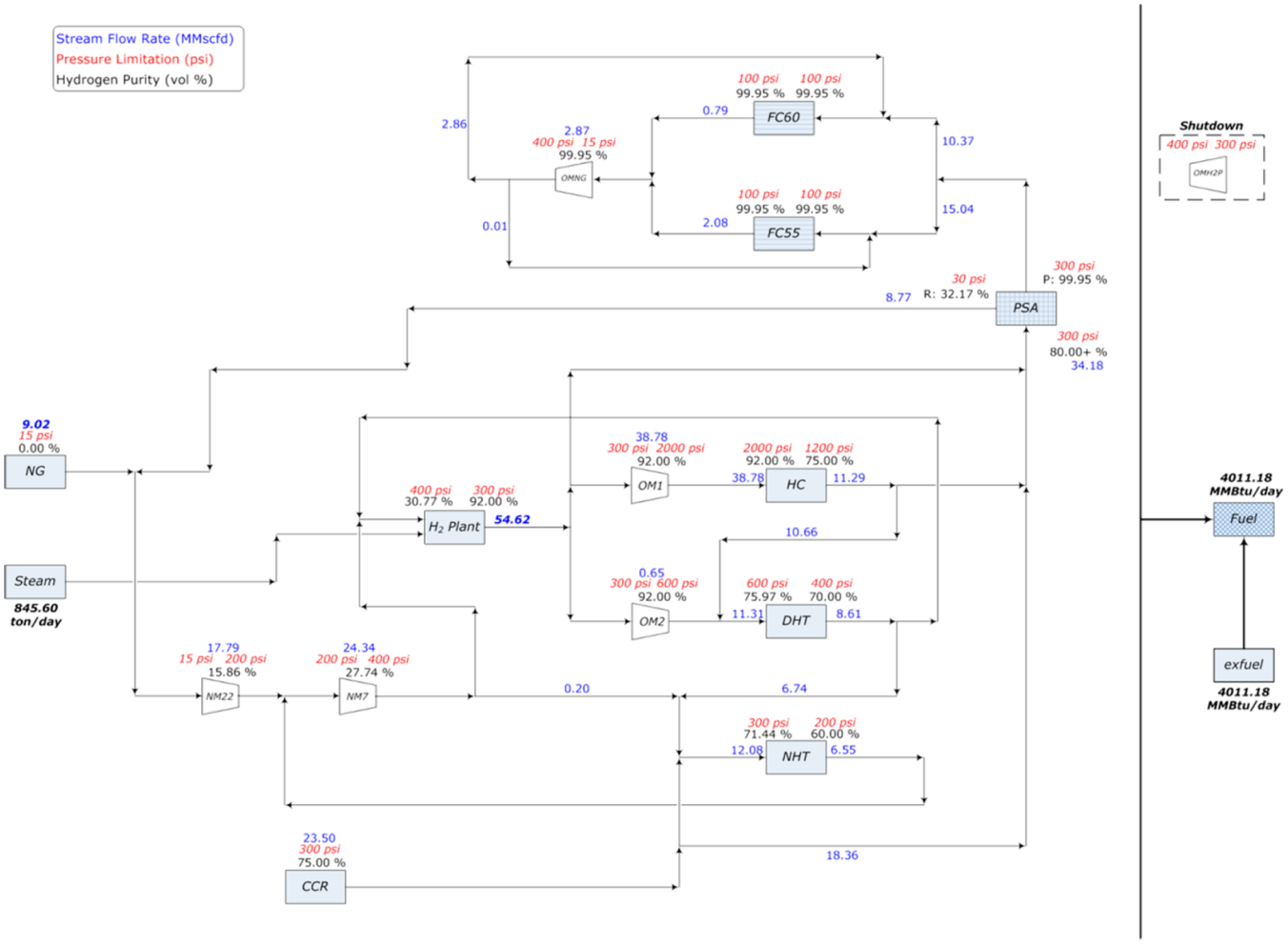

Figure 7. The multiobjective design No. 6 in Example 2.

dx.doi.org/10.1021/ie404068p | Ind. Eng. Chem. Res. 2014, 53, 6006−6020

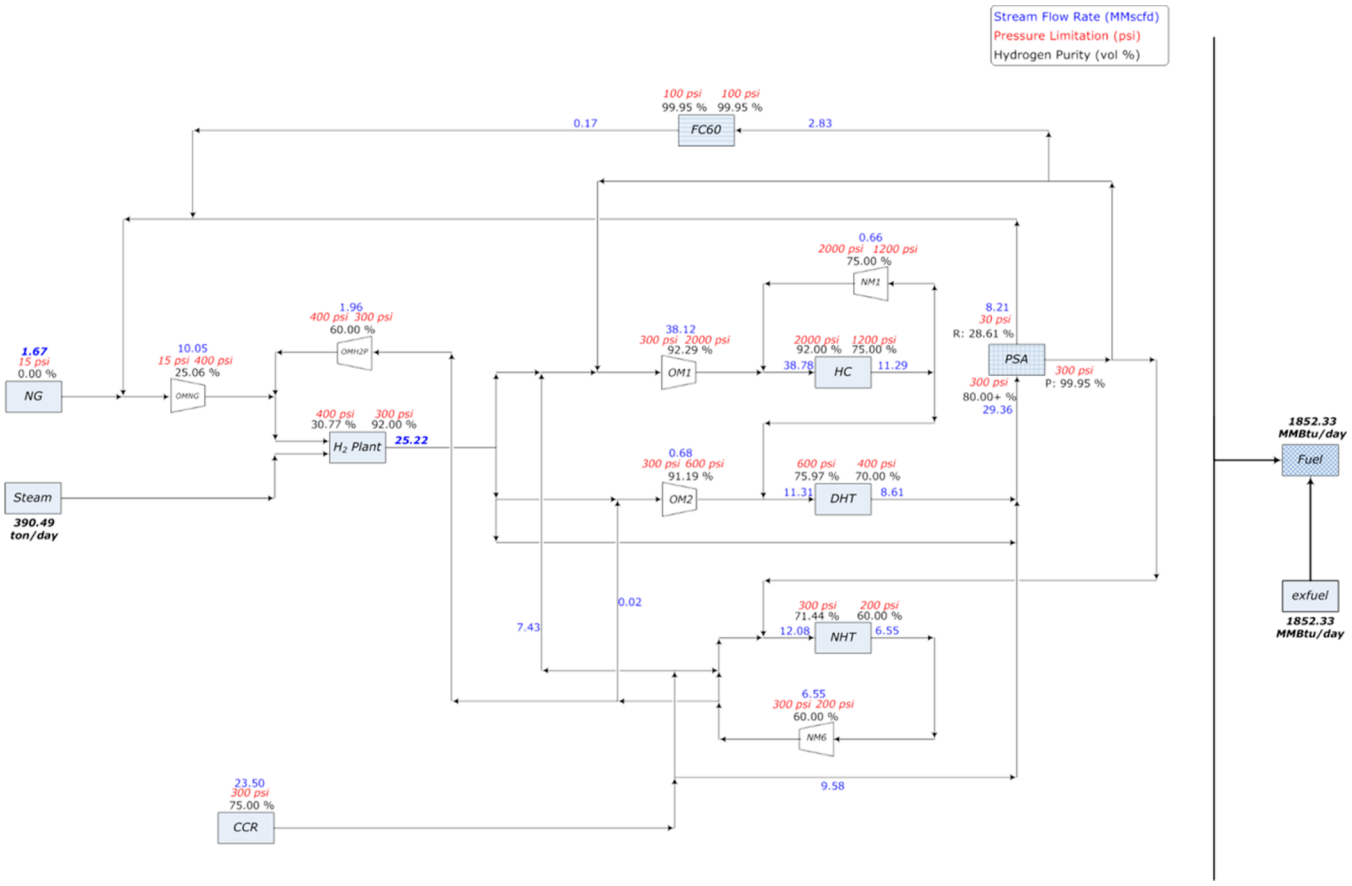

Figure 8. The multiobjective design No. 19 in Example 2.

Table 22. Power Consumption Rates of Compressors and Power Generation Rates of Fuel Cells in Multiobjective Design No. 6 of Example 2

compressor	OM1	OM2	OMNG	OMH2P	NM7	NM22
power (MW)	2.42	0.01	0.40	0.00	0.44	1.54
fuel cell	FC60	FC55				
power (MW)	15.00	15.63				

Table 23. Power Consumption Rates of Compressors and Power Generation Rate of Fuel Cell in Multiobjective Design No. 19 of Example 2

compressor	OM1	OM2	OMNG	OMH2P	NM1	NM6
power (MW)	2.38	0.01	1.22	0.02	0.01	0.07
fuel cell	FC60					
power (MW)	3.21					

in Figure 6, it is clear that the latter approach is in general better suited for producing the complete front in the present example. Consequently, only the corresponding objective values are reported in Table 19. The cost breakdowns and emission contributions of the base case and also five Pareto optima (i.e., No. 2, No. 6, No. 11, No. 15, and No. 19 in Table 19) are also presented in Table 20 and Table 21, respectively. Note that all multiobjective designs outperform the conventional one not only in terms of TAC but also emission rate. In other words, the latter should be regarded as a "dominated" solution.

It can be observed from Table 20 that the total operating cost can be lowered significantly (even to a negative value) by increasing the capital investment. This is mainly due to the fact that the profit brought about by exporting power generated by the fuel cells offsets and exceeds the increases in all other operating costs. Because of the favorable electricity price adopted in the present example, a cost-optimal design tends to call for the heaviest capital investment. However, increasing the electricity output (and the spending for fuel cells) inevitably raises the demands for hydrogen from the H_2 plant and, also, the local and global CO_2 emission rates. Although such a trend can be clearly observed in Table 21, all multiobjective optimal solutions are still less polluting than the base-case scenario.

As examples, Figure 7 and Figure 8 show the hydrogen networks associated with two optimal solutions in Table 19, that is, No. 6 and No. 19, respectively. Note that, while cost reduction is the emphasis of former design, pollution control is stressed in the latter. A common trait can nonetheless be identified from these two structures, the tail gases from HC, DHT, and NHT are all recycled and reused for efficient H_2 utilization. Let us consider two instances of this feature: (1) In Figure 7, the output of unit DHT is reused in NHT and also recycled to the hydrogen plant. (2) In Figure 8, the output of DHT is purified in PSA and then recycled.

Notice also that, to bring down the TAC, the network in Figure 7 is equipped with two fuel cells, FC60 (η_{fc} = 0.60) and FC55 (η_{fc} = 0.55), so as to generate the largest amount of electricity. The extra compressors (NM7 and NM22) in this case are installed mainly to satisfy the need for a relatively high throughput. On the other hand, only one fuel cell, FC60 (η_{fc} =

dx.doi.org/10.1021/ie404068p | Ind. Eng. Chem. Res. 2014, 53, 6006−6020

0.60), is needed in the more environmentally conscious design (see Figure 8). The extra compressors (NM1 and NM6) are chosen in this structure primarily for recycling the tail gases from HC and NHT. For the sake of completeness, the power consumption and generation rates in compressors and fuel cells in the above two designs are presented in Table 22 and Table 23, respectively.

CONCLUSIONS AND FUTURE WORKS

By incorporating the unit models of extra fuel cells, PSAs, and compressors, a comprehensive mixed-integer nonlinear program has been developed in this work to optimally integrate the hydrogen resources in any given refinery. Both single- and multiobjective designs can be generated to address concerns for cost reduction and pollution abatement. Clearly, the designer is provided with an excellent opportunity to identify the most appropriate solution from the numerous candidates located on the Pareto front. The effectiveness of this design strategy is confirmed in two case studies presented in this paper and also additional ones in Chiang.[30]

While the proposed approach is quite promising, there are still a few problems for future study. First of all, the unit models may be modified to better describe the realistic operations; for example, it is more reasonable to treat the inlet and outlet flow rates and hydrogen concentrations of hydrogen users (e.g., hydrocrackers and hydrotreaters) as variables. Although this deficiency was partially fixed by Jiao et al.,[31] further improvements are still necessary. Second, the cleaner alternatives to produce hydrogen (e.g., see Wu et al.[32]) in a hydrogen network should be evaluated. Note that, although operating a fuel cell does not cause CO_2 emission, the steam reforming process that produces its raw material (hydrogen) does. Finally, the design objectives considered in this work may be combined into a single one in the future after the carbon taxation and trade systems become mature enough for practical applications.

AUTHOR INFORMATION

Corresponding Author

*E-mail: ctchang@mail.ncku.edu.tw.

Notes

The authors declare no competing financial interest.

NOMENCLATURE

Indices

COM = set of all compressors
COM′ = set of new compressors (**COM′**⊂**COM**)
CS = set of hydrogen users
FC = set of all fuel cells
FC′ = set of new fuel cels (**FC′**⊂**FC**)
I = set of sources
J = set of sinks
NEQ = set of new equipment (**NEQ**=**COM′**∪**PUR′**∪**FC′**)
PUR = set of all purifiers
PUR′ = set of new purifiers (**PUR′**⊂**PUR**)

Variables

C = capital cost
Cems = carbon dioxide emission rate (ton/day)
cost = operating cost
e = binary variable of equipment exist or not
F = flow rate (MMscfd)
f = objective function
power = electric power
Q = daily fuel value (MMBtu/day)
y = purity
StMuse = steam requirement (ton/day)

Parameters

Af = annualizing factor
a = capital cost coefficient
b = capital cost coefficient
C_p = heat capacity at constant pressure
fi = fractional interest rate
LHV = low heating value of combustion
N = numbers of new equipment
ny = number of years
oy = annual operating hours (h)
P = pressure (psi)
R = hydrogen recovery ratio
T = temperature (K)
U = price per unit quantity
$\bar{y}$ = constant hydrogen purity
ΔH_c^o = heat of combustion
γ = ratio of heat capacity at constant pressure to that at constant volume
η = efficiency

Subscripts

comp = compressor
cs = hydrogen user
fc = fuel cell
fuel = fuel system
Gcems = total carbon dioxide emission rate
H2P = hydrogen plant
i = source
in = inlet
j = sink
lo = lower bound
NG = nature gas
neq = new equipment
out = outlet
pur = pressure swing adsorption
StM = steam
TAC = total annual cost
up = upper bound

Superscripts

max = maximum
min = minimum
nor = normalization
prod = product
resid = residual

REFERENCES

(1) Towler, G. P.; Mann, R.; Serriere, A. J.-L.; Gabaude, C. M. D. Refinery hydrogen management: Cost analysis of chemically-integrated facilities. *Ind. Eng. Chem. Res.* **1996**, *35* (7), 2378−2388.
(2) Alves, J. J.; Towler, G. P. Analysis of refinery hydrogen distribution systems. *Ind. Eng. Chem. Res.* **2002**, *41* (23), 5759−5769.
(3) Zhao, Z.; Liu, G.; Feng, X. The integration of the hydrogen distribution system with multiple impurities. *Chem. Eng. Res. Des.* **2007**, *85* (A9), 1295−1304.
(4) Ding, Y.; Feng, X.; Chu, K. H. Optimization of hydrogen distribution systems with pressure constraints. *J. Clean. Prod.* **2011**, *19*, 204−211.
(5) Zhang, Q.; Feng, X.; Chu, K. H. Evolutionary graphical approach for simultaneous targeting and design of resource conservation networks with multiple contaminants. *Ind. Eng. Chem. Res.* **2013**, *52* (3), 1309−1321.

(6) Hallale, N.; Liu, F. Refinery hydrogen management for clean fuels production. *Adv. Environ. Res.* **2001**, *6* (1), 81−98.
(7) Liu, F.; Zhang, N. Strategy of purifier selection and integration in hydrogen networks. *Chem. Eng. Res. Des.* **2004**, *82* (A10), 1315−1330.
(8) Kumar, A.; Gautami, G.; Khanam, S. Hydrogen distribution in the refinery using mathematical modeling. *Energy* **2010**, *35* (9), 3763−3772.
(9) Liao, Z. W.; Wang, J. D.; Yang, Y. R.; Rong, G. Integrating purifiers in refinery hydrogen networks: A retrofit case study. *J. Clean. Prod.* **2010**, *18* (3), 233−241.
(10) Ahmad, M. I.; Zhang, N.; Jobson, M. Modelling and optimization for design of hydrogen networks for multi-period operation. *J. Clean. Prod.* **2010**, *18* (9), 889−899.
(11) Jia, N.; Zhang, N. Multi-component optimization for refinery hydrogen networks. *Energy* **2011**, *36*, 4663−4670.
(12) Jagannath, A., Elkamel, A., and Karimi, I. A. Optimization of multi-refinery hydrogen networks. *Proceedings of the 11th International Symposium on Process Systems Engineering*, Elsevier B. V.: Amsterdam, The Netherlands, 2012; pp 1331−1335.
(13) Zhou, L.; Liao, Z. W.; Wang, J. D.; Jiang, B. B.; Yang, Y. R. Hydrogen sulfide removal process embedded optimization of hydrogen network. *Int. J. Hydrogen Energy* **2012**, *37* (23), 18163−18174.
(14) Wu, S.; Liu, G.; Yu, Z.; Feng, X.; Liu, Y.; Deng, C. Optimization of hydrogen networks with constraints on hydrogen concentration and pure hydrogen load considered. *Chem. Eng. Res. Des.* **2012**, *90* (9), 1208−1220.
(15) Wu, S.; Yu, Z.; Feng, X.; Liu, G.; Deng, C.; Chu, K. H. Optimization of refinery hydrogen distribution systems considering the number of compressors. *Energy* **2013**, *62*, 185−195.
(16) Smith, R.; Delaby, O. Targeting flue emissions. *Trans. Inst. Chem. Eng.* **1991**, *69* (A), 492.
(17) Chang, C. T.; Hwang, J. R. A multi-objective programming approach to waste minimization in the utility systems of chemical processes. *Chem. Eng. Sci.* **1996**, *51* (16), 3951−3965.
(18) Elkamel, A.; Ba-Shammakh, M.; Douglas, P.; Croiset, E. An optimization approach for integrating planning and CO_2 emission reduction in the petroleum refining industry. *Ind. Eng. Chem. Res.* **2008**, *47* (3), 760−776.
(19) Collodi, G.; Wheeler, F. Hydrogen production via steam reforming with CO_2 capture. *Chem. Eng. Trans.* **2010**, *19*, 37−42.
(20) Rajesh, J. K.; Gupta, S. K.; Rangaiah, G. P.; Ray, A. K. Multi-objective optimization of industrial hydrogen plants. *Chem. Eng. Sci.* **2001**, *56* (3), 999−1010.
(21) Posada, A.; Manousiouthakis, V. Heat and power integration of methane reforming based hydrogen production. *Ind. Eng. Chem. Res.* **2005**, *44* (24), 9113−9119.
(22) Pilavachi, P. A.; Chatzipanagi, A. I.; Spyropoulou, A. I. Evaluation of hydrogen production methods using the analytic hierarchy process. *Int. J. Hydrogen Energy* **2009a**, *34*, 5294−5303.
(23) Pilavachi, P. A.; Stephanidis, S. D.; Pappas, V. A.; Afgan, N. H. Multi-criteria evaluation of hydrogen and natural gas fuelled power plant technologies. *Appl. Therm. Eng.* **2009b**, *29* (11−12), 2228−2234.
(24) Smith, R. *Chemical Process Design and Integration*; John Wiley & Sons: Chichester, U.K. and New York, 2005.
(25) El-Halwagi, M. M. *Sustainable Design through Process Integration: Fundamentals and Applications to Industrial Pollution Prevention, Resource Conservation, and Profitability Enhancement*; Butterworth-Heinemann/Elsevier: Boston, MA, 2012.
(26) Chatzimouratidis, A. I.; Pilavachi, P. A. Multi-criteria evaluation of power plants impact on the living standard using the analytic hierarchy process. *Energy Policy* **2008**, *36* (3), 1074−1089.
(27) Jiao, Y. Q.; Su, H. Y.; Liao, Z. W.; Hou, W. F. Modeling and multi-objective optimization of refinery hydrogen network. *Chin. J. Chem. Eng.* **2011**, *19* (6), 990−998.
(28) Song, J.; Park, H.; Lee, D. Y.; Park, S. Scheduling of actual size refinery processes considering environmental impacts with multi-objective optimization. *Ind. Eng. Chem. Res.* **2002**, *41* (19), 4794−4806.
(29) Lee, J. U.; Han, J. H.; Lee, I. B. A multi-objective optimization approach for CCS infrastructure considering cost and environmental impact. *Ind. Eng. Chem. Res.* **2012**, *51* (43), 14145−14157.
(30) Chiang, Y. C. *Multi-Objective Optimal Designs for Hydrogen Networks in Petroleum Refineries with Hydrogen Plants and Fuel Cells*. MS Thesis, National Cheng Kung University, Tainan, Taiwan, 2013.
(31) Jiao, Y.; Su, H.; Hou, W. Improved optimization methods for refinery hydrogen network and their applications. *Control Eng. Practice* **2012**, *20* (10), 1075−1093.
(32) Wu, W.; Liou, Y. C.; Zhou, Y. Y. Multi-objective optimization of a hydrogen production system with low CO_2 emissions. *Ind. Eng. Chem. Res.* **2012**, *51*, 2644−2651.